ELSEVIER

Journal of Chromatography A, 814 (1998) 83–95

JOURNAL OF CHROMATOGRAPHY A

Structural characteristics of low-molecular-mass displacers for cation-exchange chromatography

Abhinav A. Shukla[a], Kristopher A. Barnthouse[a], Sung Su Bae[b], J.A. Moore[b], Steven M. Cramer[a,*]

[a]*Department of Chemical Engineering, Rensselaer Polytechnic Institute, Troy, NY 12180, USA*
[b]*Department of Chemistry, Rensselaer Polytechnic Institute, Troy, NY 12180, USA*

Received 12 March 1998; received in revised form 1 May 1998; accepted 1 May 1998

Abstract

The relative efficacy of a variety of low-molecular-mass displacers was examined using a displacer ranking plot. This method enables an evaluation of the dynamic affinity of a variety of displacers over a range of operating conditions. Several homologous series of molecules were evaluated to provide insight into the effects of various structural features on displacer efficacy. The results indicate that linear flexible geometries may have advantages over branched or cyclic structures. Data also indicate that the spreading out of charges may increase affinity. The incorporation of aromatic moieties in these displacers, particularly near the surface of the molecules, appears to result in a dramatic increase in displacer affinity. The ability of several high-affinity low-molecular-mass displacers to displace a very strongly bound cationic protein is also examined. The results confirm the predictions of the theory and indicate that it is indeed possible to displace highly bound macromolecules with low-molecular-mass displacers. The work presented in this paper indicates that non-specific interactions can be exploited for producing high-affinity low-molecular-mass displacers.

Keywords: Displacement chromatography; Displacers; Cation-exchange displacers

1. Introduction

Displacement chromatography has attracted significant attention over the past decade for its potential as a high-resolution/high-throughput purification process [1–5]. Recent reports have demonstrated the efficacy of displacement chromatography for the purification of proteins from industrial process streams [6,7].

Conventionally, large polyelectrolytes have been employed as displacers for ion-exchange systems [8–11]. An important recent advance has been the discovery that low-molecular-mass displacers can also be employed as effective displacers [12]. A variety of low-molecular-mass displacers have been identified including protected amino acids [12], dendrimers [13], and antibiotics [14]. Furthermore, low-molecular-mass displacers have been successfully employed for high resolution separations [15].

Low-molecular-mass displacers have significant operational advantages as compared to large polyelectrolyte displacers and have generated significant interest from the industry. First and foremost, if there is any overlap between the displacer and the protein

*Corresponding author.

0021-9673/98/$19.00
PII: S0021-9673(98)00374-4

of interest, these low-molecular-mass materials can be readily separated from the purified protein during subsequent downstream processing involving size-based purification methods. The relatively low cost of synthesizing low-molecular-mass displacers can be expected to significantly improve the economics of displacement chromatography. Furthermore, the salt dependent adsorption behavior of these low-molecular-mass displacers greatly facilitates column regeneration. The use of low-molecular-mass displacers also opens up the possibility of performing selective displacement chromatography [6,16].

While low-molecular-mass displacers have been successfully employed for protein purification in ion-exchange systems, to date these displacers have possessed moderate affinities and have been unable to displace highly retained biomolecules. Thus, there is a need for high affinity, low-molecular-mass displacers that would enable a wide range of displacement separations.

It has been recognized that linear retention in ion-exchange chromatography is not based solely on electrostatic interactions [17–21] but may also be affected by hydrogen bonding, hydrophobic interactions, and steric effects. However, to date, there has been a lack of knowledge about the specific structural characteristics of a molecule that determine its affinity in ion-exchange systems.

In this paper, the relative efficacy of a variety of low-molecular-mass displacers is examined using a displacer ranking plot. This method enables an evaluation of the dynamic affinity of a variety of displacers over a range of operating conditions. Several homologous series of molecules are studied using this approach to provide insight into the effects of various structural features on displacer efficacy.

2. Theory

The steric mass action (SMA) model [22] can successfully predict complex behavior in ion-exchange systems. Here the SMA model is employed to develop a framework for ranking displacer efficacy.

The SMA model involves three parameters: the characteristic charge (ν) which is the average number of sites that a molecule interacts with on a surface; the equilibrium constant (K) and the steric factor (σ) which is the average number of sites on the surface which are sterically shielded by the molecule. These SMA parameters can be readily determined using standard chromatographic procedures.

The dynamic affinity of a given component ''a'' in a displacement separation is given by [22]:

$$\lambda_a = \left(\frac{K_a}{\Delta}\right)^{1/\nu_a} \tag{1}$$

where ν_a and K_a are the characteristic charge and the equilibrium constant respectively for component ''a'' and Δ is the partition ratio of the displacer ($\Delta = Q_d / C_d$) where Q_d and C_d are the displacer concentrations in the stationary phase and the mobile phase, respectively.

Taking the logarithm of both sides of Eq. (1) yields:

$$\log K_a = \log(\Delta) + \log(\lambda_a)\nu_a \tag{2}$$

Thus a plot of $\log K_a$ vs. ν_a (dynamic affinity plot, [23]) defines two regions demarcated by a line with a slope equal to $\log \lambda_a$ and intercept of $\log \Delta$. The line originates at the point $\log(\Delta)$ on the y-axis and passes through the point defined by the parameters K_a and ν_a of the species ''a''. The region above the affinity line includes all solutes which will displace ''a'' when traveling at a velocity defined by Δ. Conversely the solutes in the region below the affinity line will be displaced by ''a'' under these conditions. Because this plot can be used to determine the elution order of components in a displacement train, it may be used to compare displacer efficacies to each other under a specific set of operating conditions (i.e., salt and displacer concentrations).

To enable a comparison over a range of operating conditions, the dynamic affinity λ (which is the criterion for displacement) can be plotted against the displacer partition ratio Δ (which is the operating variable for displacement). The equation for such a plot can be determined by rearrangement of Eq. (2) as:

$$\log(\lambda_a) = \frac{1}{\nu_a}\log K_a - \frac{1}{\nu_a}\log(\Delta) \tag{3}$$

Thus, a plot of $\log(\lambda_a)$ vs. $\log(\Delta)$ (Fig. 1) can be constructed using the linear SMA parameters of a displacer. For a given Δ value, the higher the λ_a value, the better the displacer under those operating conditions. As is expected, an increase in the Δ value as one moves along the *x*-axis (which corresponds to lower displacer concentrations or lower salt concentrations) results in a decrease in the value of the dynamic affinity (λ_a). This plot can be effectively employed to rank the relative efficacy of displacers. In contrast to the dynamic affinity plot which is constructed for a fixed value of Δ, this ranking plot can show the variation of the dynamic affinity of a molecule over a range of Δ values. Thus, in Fig. 1, while solute 1 has a higher dynamic affinity over a range of Δ from 1 to 10, solute 2 has a higher dynamic affinity for values of $\Delta > 10$.

3. Experimental

3.1. Materials

Strong cation-exchange (SCX, 8 mm, 100×5 mm I.D.) and strong anion-exchange (SAX, 8 mm, 100×5 mm I.D.) columns were obtained from Waters (Milford, MA, USA). A Zorbax C_3 reversed-phase column (250×4.6 mm I.D.) was obtained from BTR Separations (Wilmington, DE, USA). Sodium sulfite, guanidine·HCl, tetramethyl ammonium chloride, trimethylamine·HCl, dimethylamine·HCl, methylamine·HCl, aniline·HCl, butylamine, benzylamine·HCl, 1,4,8,11-tetrazacyclotetradecane, diethylene triamine, triethylene tetramine, tetraethylene pentamine, silver oxide and catechol were from Aldrich (Milwaukee, WI, USA) and were used as

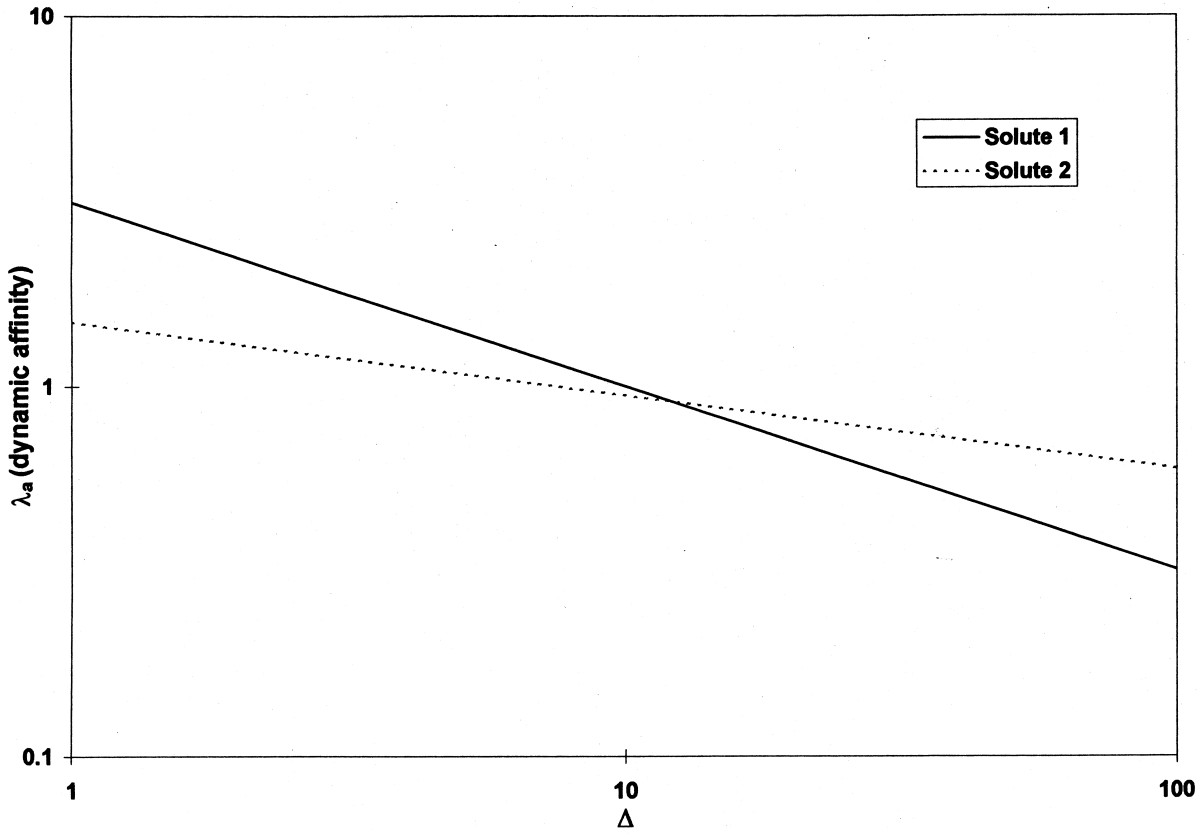

Fig. 1. Representative displacer ranking plot for two solutes. Parameters: solute 1 ($\nu=2$, $K=10$); solute 2 ($\nu=4$, $K=5$).

received. Sodium monobasic phosphate, sodium dibasic phosphate, bromophenol blue, fluorescamine, spermine and spermidine were purchased from Sigma (St. Louis, MO, USA). PETMA [pentaerythrityl(trimethylammonium (4))], DPE-TMA [dipentaerythrityl(trimethylammonium (b))], Ph-TMA [phenyldipentaerythrityl(trimethylammonium (b))], pentaerythrityl tetramine and PE-PhTMA [pentaerythrityl(benzyl, dimethylammonium (4)) chloride] were synthesized in the Department of Chemistry [25]. Recombinant human brain derived neurotrophic factor (rHuBDNF) was donated by Regeneron Pharmaceutical (Rensselaer, NY, USA).

3.2. Apparatus

All displacement experiments were carried out using a Model 590 programmable HPLC pump (Waters) connected to the chromatographic columns via a Model C10W 10-port valve (Valco, Houston, TX, USA). Data acquisition and processing were carried out using a 820 Maxima chromatography workstation (Waters) and a Millenium 2010 chromatography workstation (Waters). Fractions of the column effluent were collected using an LKB 2212 Helirac fraction collector (LKB, Sweden). Protein and displacer analysis for the collected fractions were carried out using a WISP Model 712 autoinjector (Waters) connected to a Model 650E advanced protein purification system (Waters) with a Model 484 tunable-absorbance detector (Waters). Fluorescence absorbances were measured on a LS50B spectrofluorometer (Perkin-Elmer, Wilton, CT, USA). UV absorbance of samples was measured

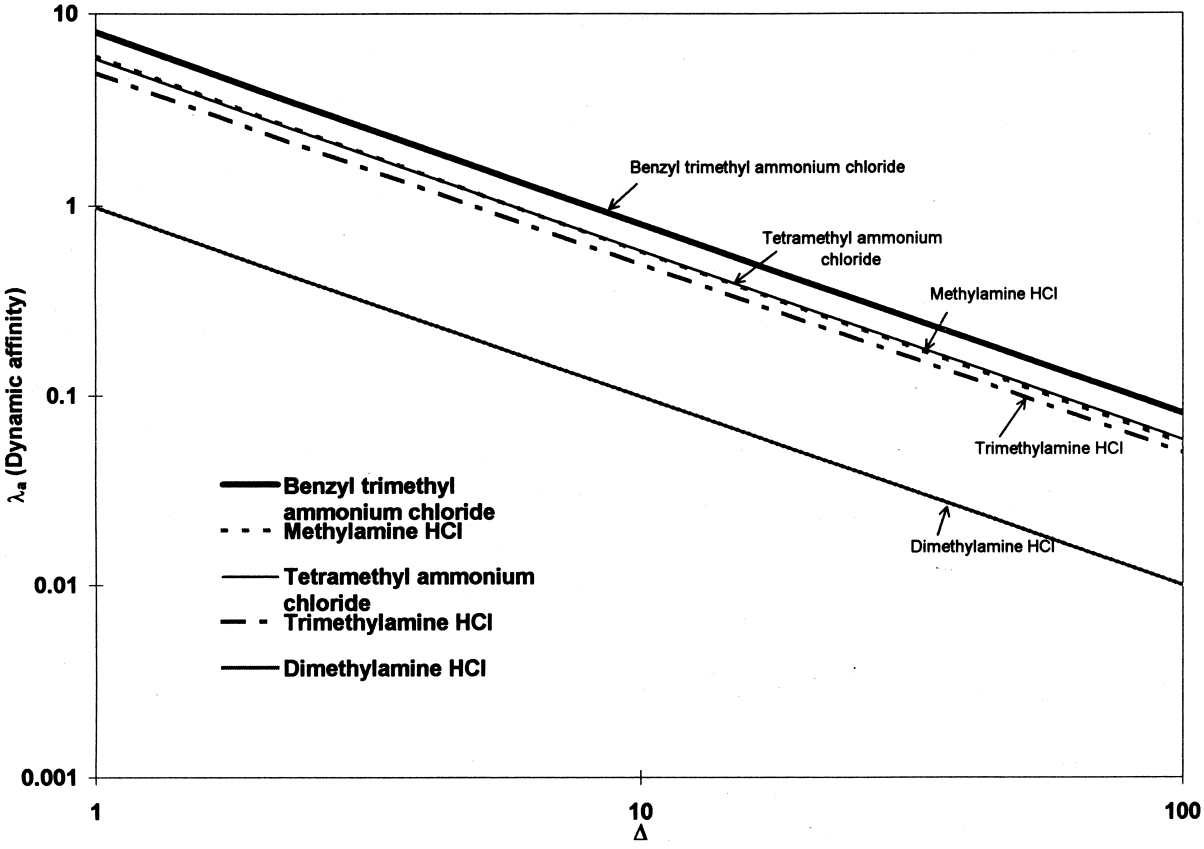

Fig. 2. Ranking of functional moieties for cation-exchange displacers. Parameters: tetramethyl ammonium chloride ($\nu=1$, $K=5.84$); trimethyl ammonium hydrochloride ($\nu=1$, $K=4.94$); dimethyl ammonium hydrochloride ($\nu=1$, $K=0.99$); methylamine hydrochloride ($\nu=0.98$, $K=5.84$). Ionic capacity: 435.7 m*M*.

on a Lambda 6 UV–Vis spectrophotometer (Perkin-Elmer).

3.3. Procedures

3.3.1. Determination of SMA parameters for displacer molecules and proteins

The characteristic charge (ν) was determined from the induced salt gradients produced during non-linear frontal experiments. The same experiments also furnished the breakthrough volumes of the displacer which were used to calculate the steric factor (σ) [24]. The equilibrium constant was fitted to the retention volumes of the displacers during linear gradient elution [25]. A minimum of three gradient lengths were employed to estimate the equilibrium constant.

3.3.2. Displacer analysis

Wherever possible, UV–Vis absorption was used to monitor the elution of the displacer molecules during linear gradient experiments. The retention volumes of other displacers were found by collecting fractions during the linear gradient elution of the displacers and subsequent estimation of the displacer in these fractions.

Primary amine containing displacers were determined by complexation with fluorescamine [26,27]. The fractions containing the displacer were diluted such that the resulting concentration of amine moieties was in the range of 0.01–0.1 m*M*. A 0.28 mg/ml solution of fluorescamine in acetone was added to the fraction containing displacer in a 1:3 (v/v) ratio. Excitation at 390 nm and emission at 475 nm were then employed to quantitate the amount of displacer in the fractions.

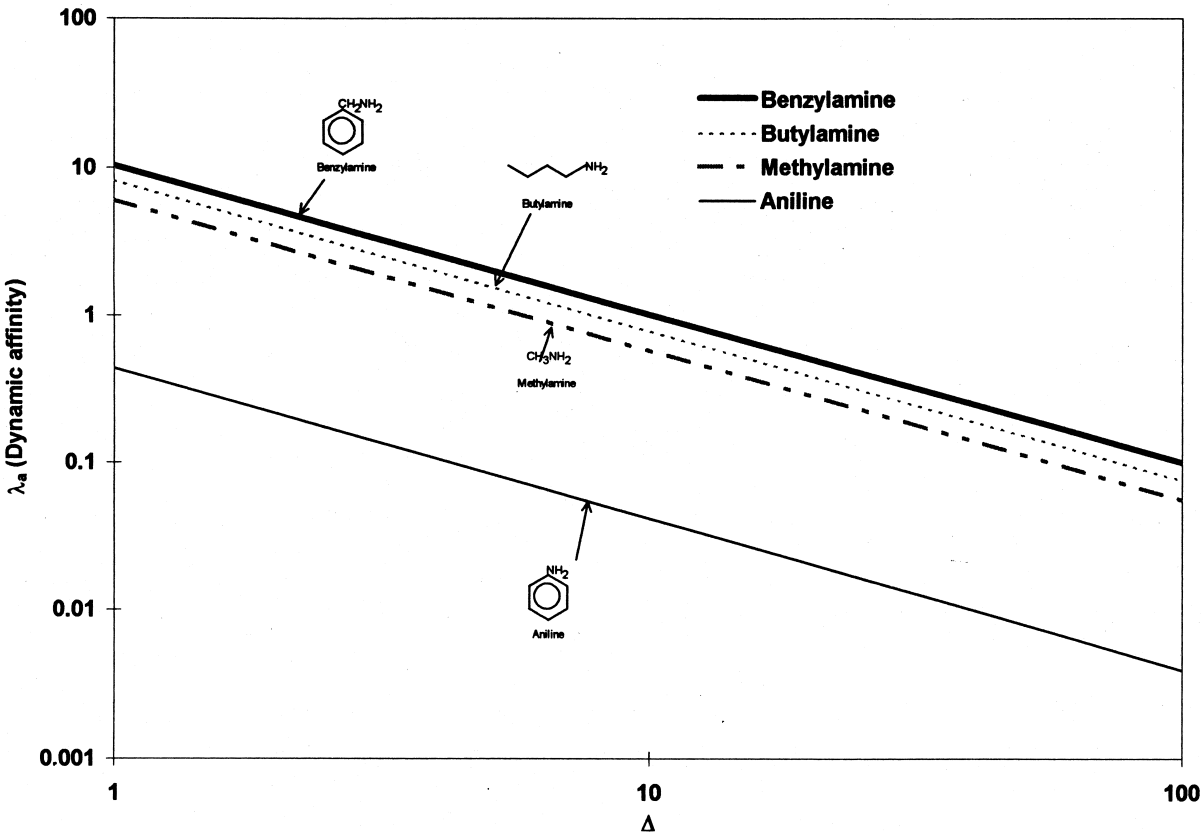

Fig. 3. Effect of hydrophobicity and aromaticity for cation-exchange displacers. Parameters: aniline hydrochloride (ν=0.97, K=0.45); butylamine (ν=0.98, K=7.84); methylamine hydrochloride (ν=0.98, K=5.84); benzylamine (ν=0.99, K=10.1).

Quaternary ammonium containing displacers were determined by complexation with bromophenol blue followed by extraction of the complex [28]. The displacer fractions were diluted to a range of 0.5–2 m*M* and mixed with 0.1 ml of 10% (w/v) Na_2CO_3 and 1 ml of 0.4 mg/ml bromophenol blue (made in 0.01 *M* NaOH). The contents of the tube were mixed to ensure a complete reaction. The complex was then extracted by 2 ml chloroform over a period of 1–2 h. The absorbance of the aqueous layer was then recorded at 590 nm. The absorbance of the aqueous layer is inversely related to the concentration of the quaternary ammonium compound in the sample.

Secondary amine-containing molecules were estimated by a complexation reaction with pyrocatechol and silver oxide [29]. The fractions were diluted to a range of 0.1 and 1 m*M* of the displacer. To a 1 ml solution of these diluted fractions, 1 ml of 1% catechol solution in acetone was added. Twenty mg of silver oxide was then added to each tube followed by mixing. The absorbance was read at 510 nm with any further dilutions required being made with acetone.

3.3.3. Operation of displacement chromatography

Displacements of the rHuBDNF were carried out on the SCX (100×5 mm, Waters SP-8HR) column. In all displacement experiments, the column was initially equilibrated with the carrier and then sequentially perfused with feed, displacer and regenerant solutions. The displacer solution was prepared in the same buffer as the carrier. Fractions of the column effluent were collected directly from the column outlet to avoid extra-column dispersion of the purified components.

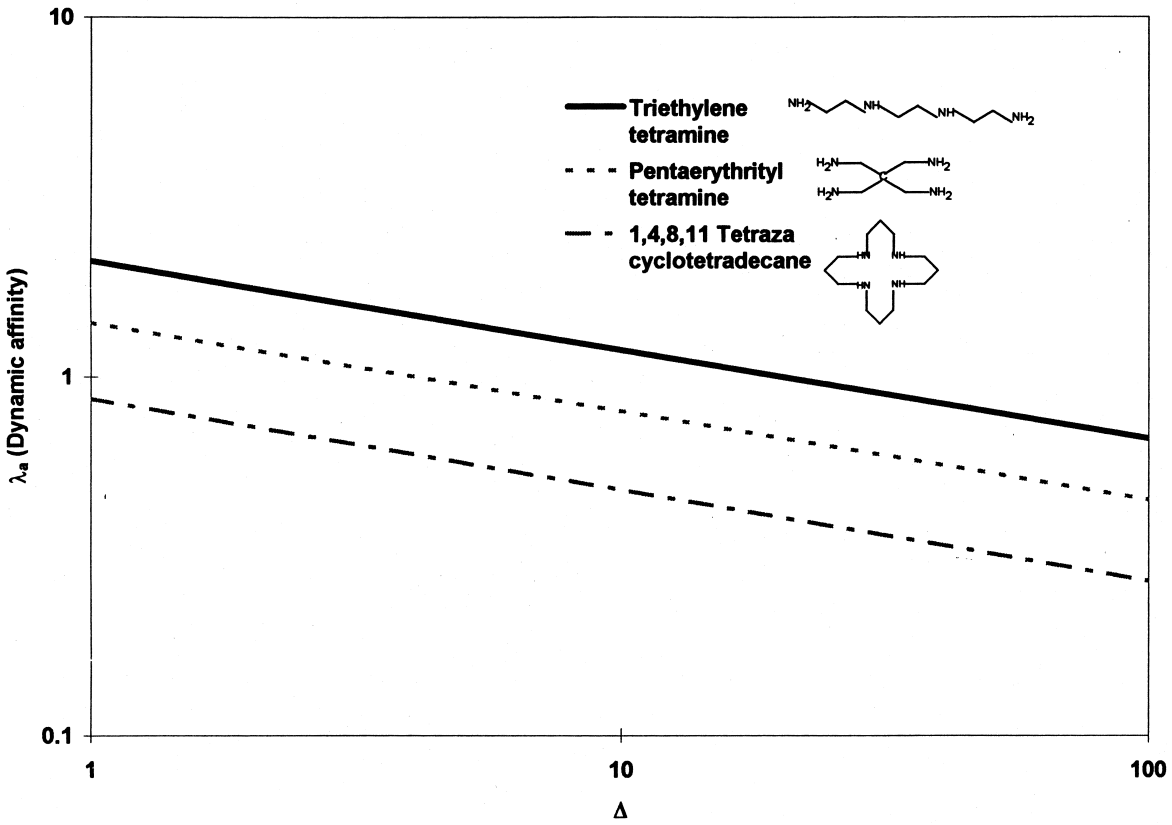

Fig. 4. Effect of molecular geometry on cation-exchange displacers. Parameters: triethylene tetramine ($\nu=4$, $K=20$); pentaerythrityl tetramine ($\nu=4$, $K=4.12$); 1,4,8,11-tetrazacyclotetradecane ($\nu=3.9$, $K=0.58$).

3.3.4. Protein analysis by high-performance liquid chromatography

rHuBDNF was analyzed by reversed-phase liquid chromatography (RPLC) on a Zorbax C_3, 250×4.6 mm I.D. column using a linear gradient from 18% acetonitrile (ACN) in water with 0.1% trifluoroacetic acid (TFA) to 54% ACN in water with 0.1% TFA in 25 min. A flow-rate of 1 ml/min was used and the effluent monitored at 237 nm. The same assay was employed to quantify PE-DMABzCly and DPE-TMA6 in the displacement of rHuBDNF.

4. Results and discussion

The ranking plot (plot of log λ_a vs. log Δ) enables a comparison of the efficacies of various displacers over a range of operating conditions. To study the effect of various structural changes on the efficacy of low-molecular-mass displacers, several cationic molecules were arranged in homologous series. The molecules in each series differ from each other in predominantly one structural characteristic, thus ranking the efficacies of the molecules in each of these series enables one to probe the key structural characteristics of low-molecular-mass displacers.

The ranking order obtained from the ranking plot is obtained over a range of Δ values. The practical range of Δ values for a displacement on a given stationary phase can be obtained from the relation between the Δ value and the displacer breakthrough volume:

$$\Delta = \frac{Q_d}{C_d} = \frac{(V_{br} - V_0)}{(V_{col} - V_0)} \quad (4)$$

where V_{br} is the breakthrough volume of the dis-

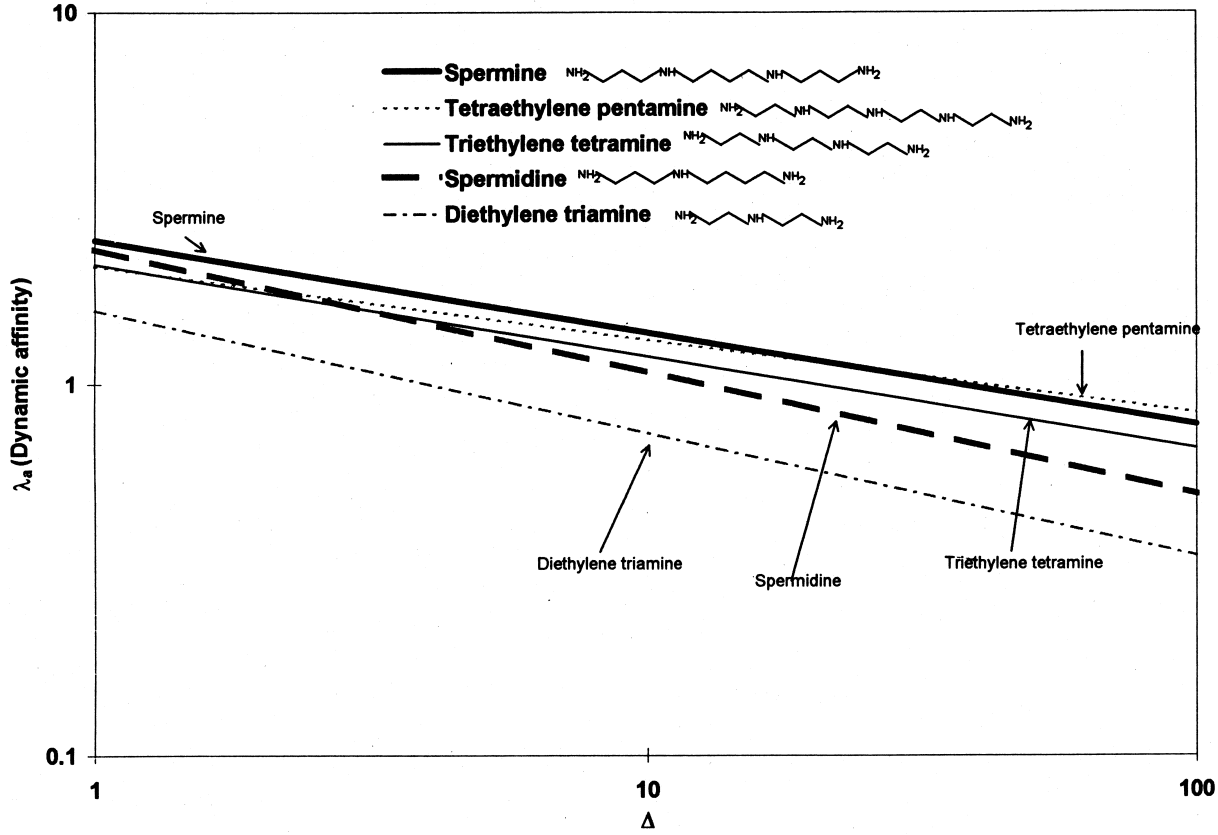

Fig. 5. Relative ranking of extended cation-exchange displacer structures. Parameters: spermine (ν=4, K=36.3); spermidine (ν=3, K=12.6); tetraethylene pentamine (ν=5, K=40.3); triethylene tetramine (ν=4, K=20); diethylene triamine (ν=3, K=4).

placer, V_0 is the void volume of the column and V_{col} is the column volume. For most displacements employing low-molecular-mass displacers, the breakthrough volumes vary from 2 to 6 void volumes. The stationary phase employed in this study has a porosity (V_0/V_{col}) of 0.73 which results in Δ values ranging from 2.6 to 13 (corresponding to the breakthrough volumes ranging from $2V_0$ to $6V_0$). Thus the relative efficacies of the displacers should be examined in this range of Δ values.

The range of practical Δ values could also be based on other factors such as protein solubility (use of a higher displacer concentration may result in concentrating the proteins beyond their solubility limit) or the magnitude of the induced salt gradient (a higher displacer concentration may lead to elution of the proteins in the induced salt gradient). Thus, the range of the operational parameter (Δ) can also be based on practical criteria depending on the particular separation problem at hand.

Fig. 2 shows the relative ranking of six functional moieties that could be used in cation-exchange displacers. These results indicate that benzyl trimethyl ammonium chloride has the highest affinity, followed by the primary amine, quaternary ammonium and tertiary amine functionalities. In contrast, the secondary amine group has a significantly lower affinity. The basicity of the amines has been shown to follow the order $4°>3°>2°>1°$ [30,31] primarily due to the inductive effect of the methyl groups. On the other hand, the steric hindrance to the approach of charge to a surface has been shown to follow the order $4°>3°>2°>1°$ [32]. Hydrophobic/aromatic effects have also been found to be important for the

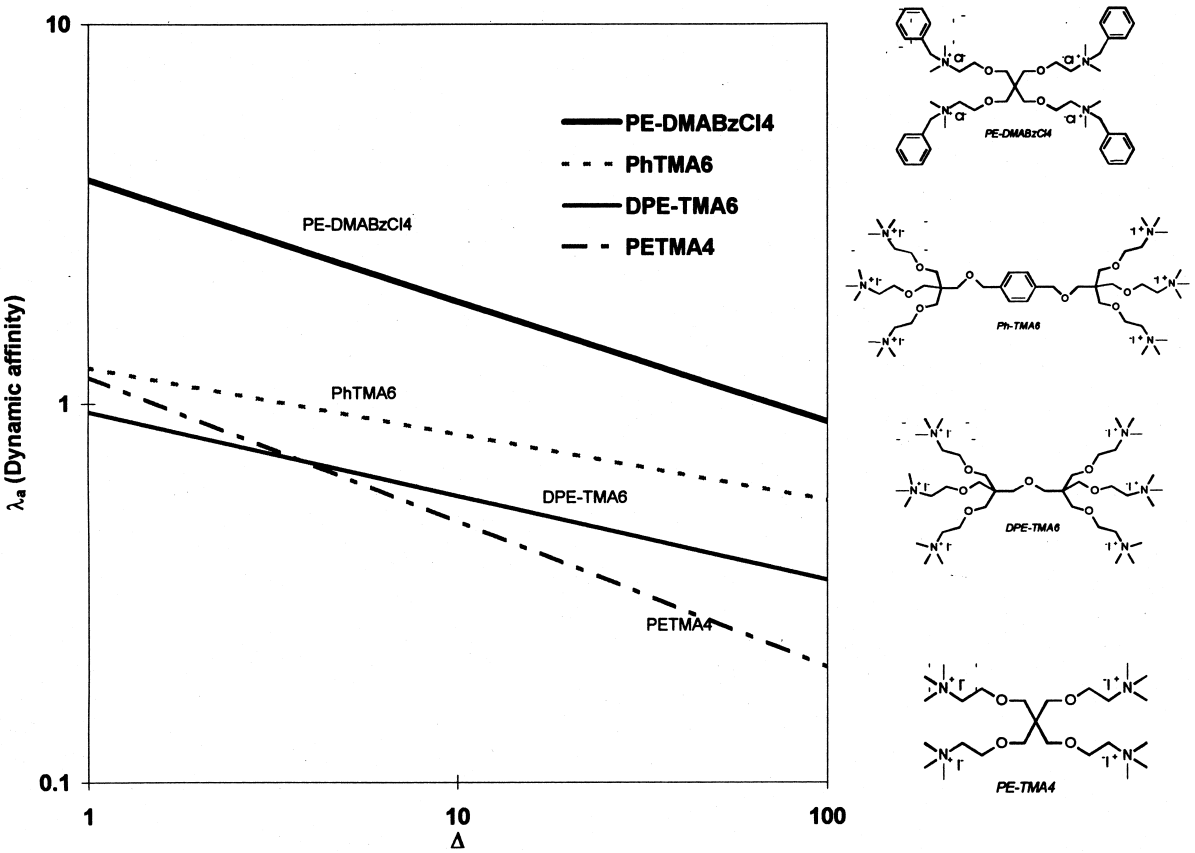

Fig. 6. Relative ranking of branched cation-exchange displacer structures. Parameters: PETMA4 ($\nu=2.6$, $K=1.52$); PE-DMABzCl4 ($\nu=3.12$, $K=70.2$); DPE-TMA6 ($\nu=4.47$, $K=0.79$); PhTMA6 ($\nu=5.65$, $K=3.47$).

chromatographic elution order of amines. In RPLC, the order was seen to depend on the number of alkyl groups on the N atom [33]. The hydrophobic effect could well account for the greater efficacy of the benzyl substituted quaternary ammonium ion. Clearly, the ranking order shown in Fig. 2 results from an interplay of several factors including the basicity of the molecule, steric hindrance to the approach of charges to the stationary phase, and aromaticity/hydrophobicity effects.

The importance of aromatic/hydrophobic interactions for displacer molecules can be seen from the comparison in Fig. 3. Here the order of effectiveness is benzylamine>butylamine>methylamine>aniline. Clearly the aromatic/hydrophobic interactions in butylamine and benzylamine enhance the effectiveness of these molecules. However, the affinity is not determined solely by the hydrophobicity. While aniline has essentially the same hydrophobicity as benzylamine, it has a markedly lower affinity due to its lower basicity, which results from the electron withdrawing nature of the benzene ring [34].

Molecular geometry is another important criterion for displacer design. Fig. 4 shows a comparison of linear, branched and cyclic structures, each with four charges. As seen in the figure, the linear structure is superior to the branched and cyclic structures. This increased affinity is probably due to the greater flexibility associated with a linear chain, resulting in a better orientation with the stationary phase surface.

Fig. 5 shows a comparison of several linear molecules. As seen in the figure, increasing the number of charges (e.g., tetraethylene pentamine> triethylene tetramine>diethylene triamine, or spermine>spermidine) improves the efficacy of these linear displacers. Another interesting effect is

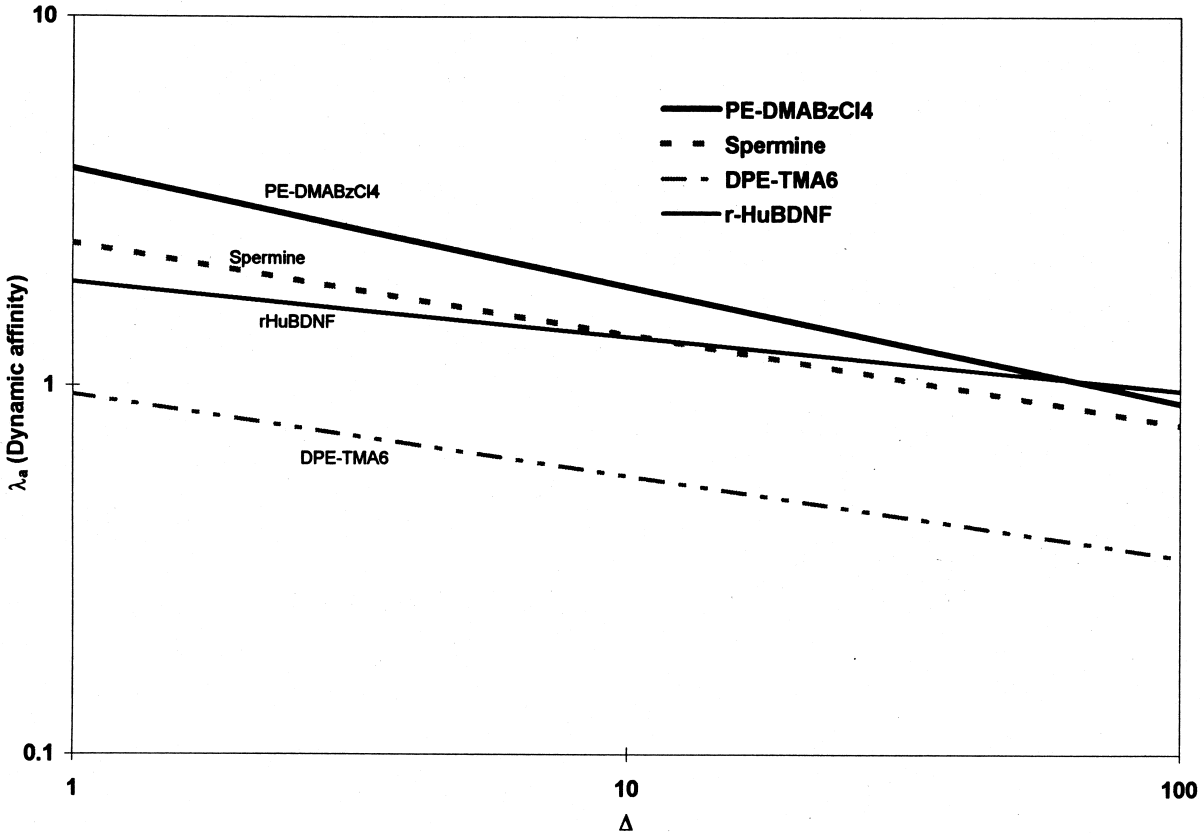

Fig. 7. Log λ_a vs. log Δ plot for the displacers PE-DMABzCly, spermine and DPE-TMA6 along with the protein rHuBDNF. Parameters: rHuBDNF ($\nu=6.72$, $K=79.7$); displacer parameters as listed earlier.

that of the spacing between the charges. It turns out that the greater the spacing between the charges, the higher the affinity of the displacers. For example, while spermine and triethylene tetramine both have four charges, spermine has a greater spacing between the charges and a correspondingly higher affinity. Similarly, spermidine was shown to have higher affinity than diethylene triamine. This spacing effect could be due to increased flexibility of the molecule and/or greater hydrophobicity associated with the presence of additional methylene groups.

Fig. 6 shows a comparison of branched displacer structures including PETMA, DPE-TMA, Ph-TMA and PE-DMABzCl4. As described above, a reasonable operating range for displacement chromatography on this stationary phase is $2.6<\Delta<13$. Thus the order of affinity of these synthesized displacers [25] is: PETMA<DPE-TMA<Ph-TMA<PE-DMABzCl4. The increase in affinity from PETMA to DPE-TMA is primarily due to an increase in the number of charges. The higher affinity of Ph-TMA relative to DPE-TMA is possibly due to the presence of the benzene ring, which provides a higher hydrophobicity of the molecule and/or the greater spacing between the charged ends of the molecule.

The PE-DMABzCl4 displacer has a dramatically higher affinity than the other molecules even though it has only four charged moieties. This could be the result of a large increase in the overall hydrophobicity of the molecule, as well as due to the placement of benzyl moieties at the charged termini where they have the greatest possibility of interaction with the stationary phase surface. These results emphasize the importance of non-specific interactions in determining the affinity of displacers in ion-exchange chromatography.

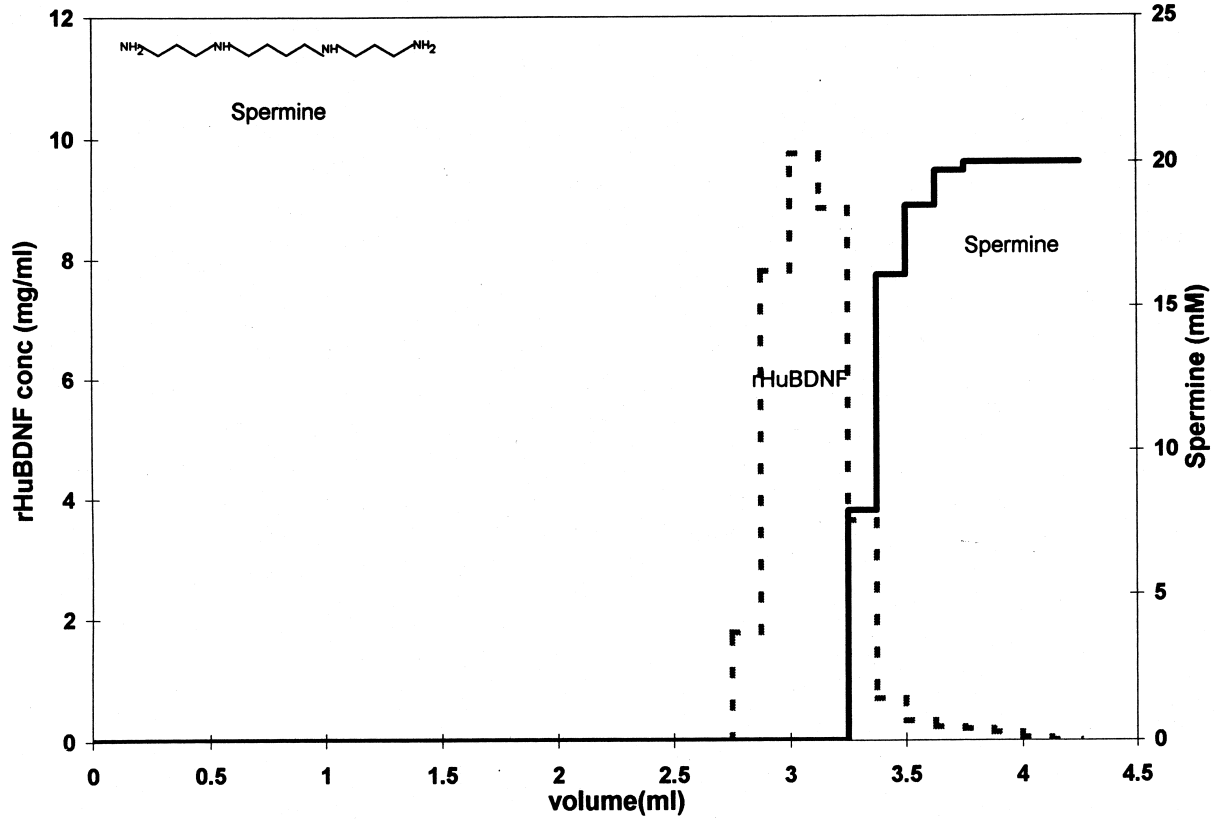

Fig. 8. Displacement of rHuBDNF by spermine. Column: Waters SP-8HR, 100×5 mm; mobile phase: phosphate buffer (Na^+ concentration: 400 m*M*), pH 6; displacer: 20 m*M* spermine; loading: 6.25 mg rHuBDNF.

rHuBDNF is a highly basic protein (pI~10.3 [35]) which is strongly retained on cation-exchange resins [7]. During gradient elution, rHuBDNF was observed to elute in salt concentrations as high as 700 mM. Fig. 7 presents the ranking plot of rHuBDNF in addition to several high affinity displacers. According to the theory, DPE-TMA6 does not possess sufficient dynamic affinity to displace rHuBDNF under any operating conditions. On the other hand, it is predicted that spermine should be able to displace rHuBDNF when $\Delta<10$. The highest affinity displacer, PE-DMABzCl4, is shown to have sufficient dynamic affinity to displace rHuBDNF over a wide range of operating conditions.

Previous work in our laboratory has shown that rHuBDNF can be successfully displaced with protamine, resulting in a separation of protein variants [7]. To date, no low-molecular-mass displacers have been able to displace the strongly-bound rHuBDNF. In order to evaluate the predictions of the ranking plot (Fig. 7) several displacement experiments were carried out. The displacement of rHuBDNF by spermine and PE-DMABzCl4 are shown in Figs. 8 and 9, respectively. (Note: these displacements were carried out at Δ values of 3.5 and 2.7, respectively). As seen in the figures, both molecules were indeed successful in displacing the rHuBDNF, verifying the predictions made by the ranking plot. These results indicate that low-molecular-mass displacers can indeed possess sufficient affinity to displace very strongly bound cationic proteins. An experiment carried out with DPE-TMA at a significantly lower Δ (=0.65) is shown in Fig. 10. In contrast to the displacements shown in Figs. 8 and 9, this experiment did not produce displacement of rHuBDNF, as predicted from the theory (Fig. 7). Thus, despite the presence of a greater number of charges, this displacer failed to displace rHuBDNF.

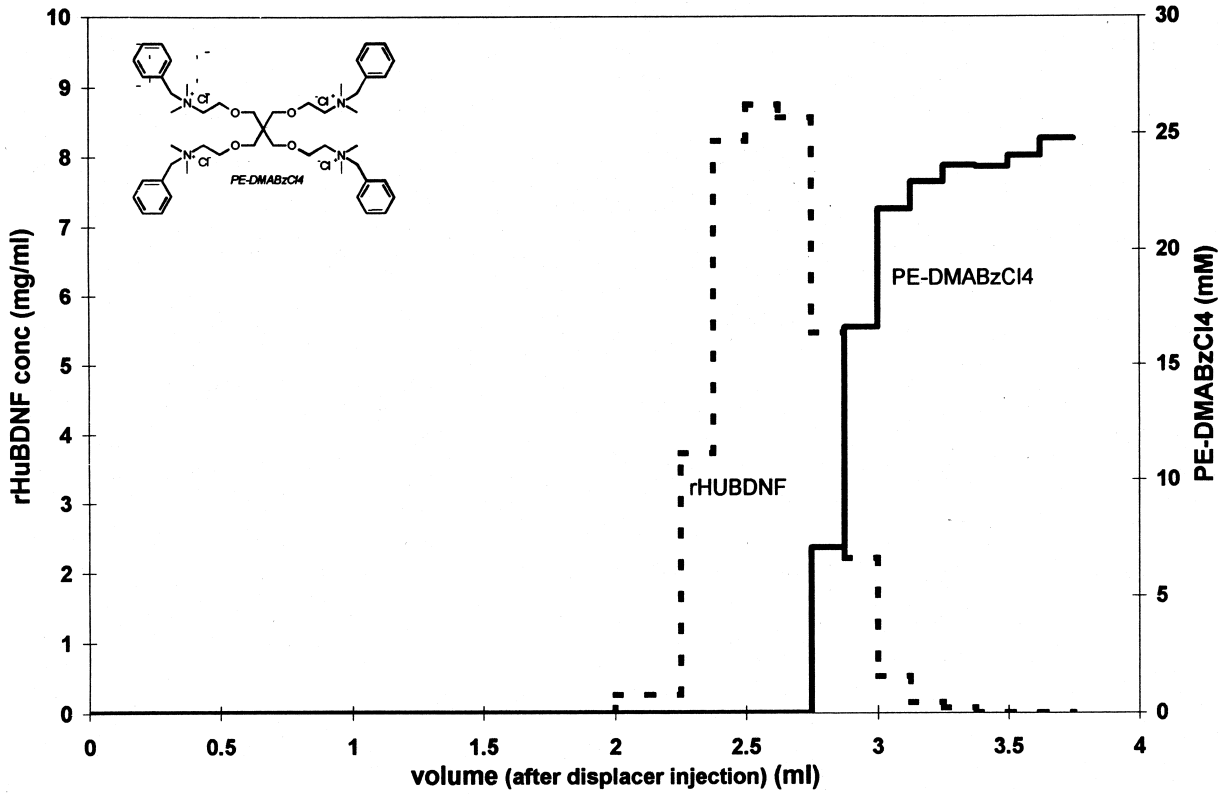

Fig. 9. Displacement of rHuBDNF by PE-DMABzCl4. Column: Waters SP-8HR, 100×5 mm; mobile phase: phosphate buffer (Na^+ concentration: 450 mM), pH 6; displacer: 25 mM PE-DMABzCl4; loading: 6.25 mg rHuBDNF.

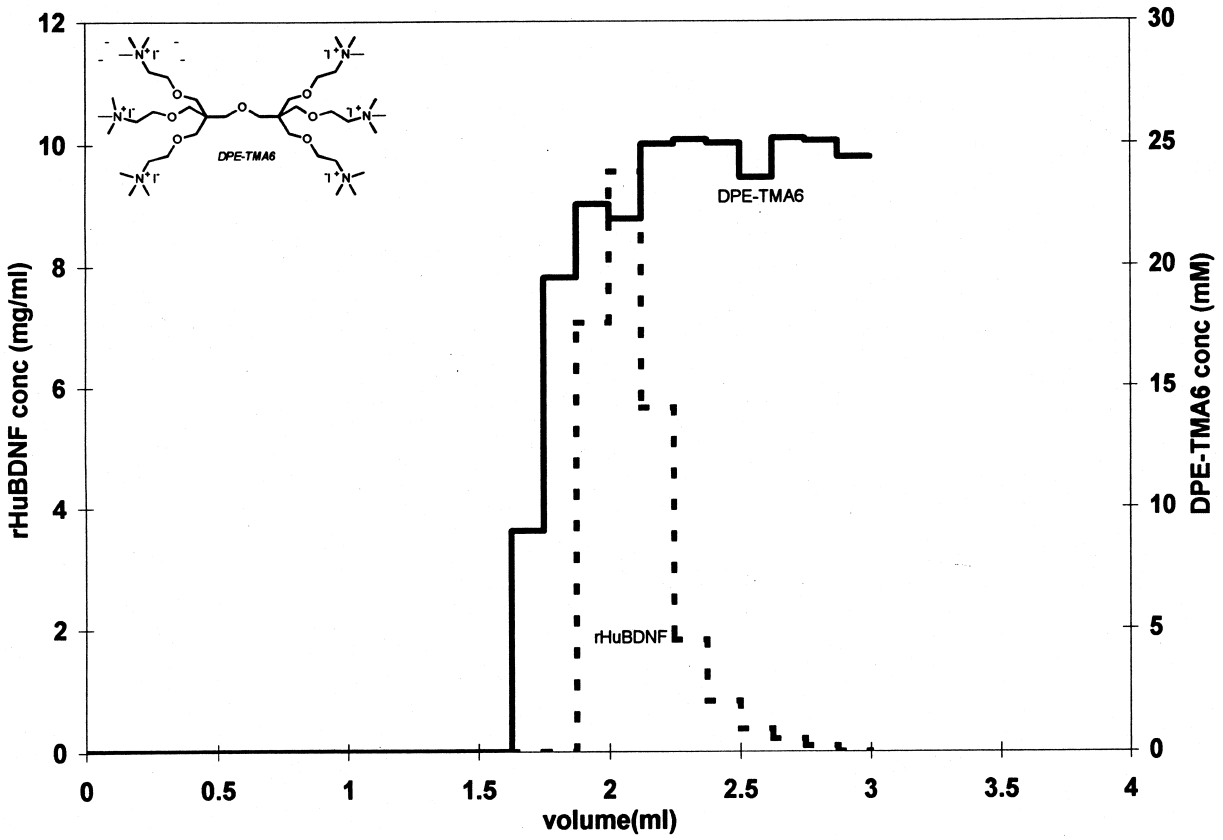

Fig. 10. Desorption of rHuBDNF by DPE-TMA6. Column: Waters SP-8HR, 100×5 mm; mobile phase: phosphate buffer (Na^+ concentration: 450 m*M*), pH 6; displacer: 25 m*M* DPE-TMA6; loading: 6.25 mg rHuBDNF.

This serves to indicate that charge is not the only factor for determining the affinity of low-molecular-mass displacers and that non-specific interactions play a significant role in determining affinity in these systems.

5. Conclusions

In this manuscript, a displacer ranking plot has been employed to rank the efficacies of several homologous series of displacer molecules. The results have pointed to certain desirable structural properties of efficient low-molecular-mass displacers, namely, linear flexible geometries and the presence of aromatic groups near the surface of the molecules. Two such displacers, spermine and PE-DMABzCl4 have been shown to possess sufficient dynamic affinity to displace a highly bound cationic protein (rHuBDNF). This is the first investigation into the effect of molecular structure on displacer efficacy and lays the foundation for the further development of high affinity low-molecular-mass displacers for cation and anion-exchange chromatography on various stationary phase materials.

Acknowledgements

This research was funded by Grant GM47372 from the National Institutes of Health. The authors acknowledge Regeneron Pharmaceutical (Rensselaer, NY, USA) for providing the rHuBDNF employed in this study; Dr. Bob MacColl and Leslie Eisele of the Wadsworth Research Center, Albany for the use of their fluorescence spectrometer; and John Scarchilli

for his assistance in developing assay procedures for amine-containing displacers.

References

[1] A.W. Liao, Z. El Rassi, D.M. LeMaster, Cs. Horvath, Chromatographia 24 (1987) 881.
[2] J. Frenz, Cs. Horvath, in: Cs. Horvath (Ed.), High Performance Liquid Chromatography – Advances and Perspectives, Academic Press, New York, 1988, pp. 212–314.
[3] G. Subramanian, M.W. Phillips, S.M. Cramer, J. Chromatogr. 439 (1988) 341.
[4] S.C.D. Jen, N.G. Pinto, J. Chromatogr. Sci. 29 (1990) 478.
[5] G. Guiochon, S.G. Shirazi, A.M. Katti, Fundamentals of Preparative and Nonlinear Chromatography, Academic Press, New York, 1994, pp. 299–322.
[6] A.A. Shukla, R.L. Hopfer, E. Bortell, D. Chakrabarti, S.M. Cramer, Biotechnol. Progr. 14 (1998) 92.
[7] K.A. Barnthouse, R. Rupp, W. Trumpeter, S.M. Cramer, J. Biotechnol., submitted for publication.
[8] J.A. Gerstner, S.M. Cramer, Biotechnol. Progr. 8 (1992) 540.
[9] G. Jayaraman, S.D. Gadam, S.M. Cramer, J. Chromatogr. 630 (1993) 53.
[10] J.A. Gerstner, S.M. Cramer, BioPharm 5 (1992) 42.
[11] E.A. Peterson, A.R. Torres, Anal. Biochem. 130 (1983) 271.
[12] A. Kundu, S. Vunnum, G. Jayaraman, S.M. Cramer, Biotechnol. Bioeng. 48 (1995) 452.
[13] G. Jayaraman, Y.F. Li, J.A. Moore, S.M. Cramer, J. Chromatogr. A 702 (1995) 143.
[14] A. Kundu, S. Vunnum, S.M. Cramer, J. Chromatogr. A 707 (1995) 57.
[15] A. Kundu, S.M. Cramer, Anal. Biochem. 248 (1997) 111.
[16] A. Kundu, K.A. Barnthouse, S.M. Cramer, Biotechnol. Bioeng. 56 (1997) 119.
[17] P.J. Twichett, A.E.P. Gorvin, A.C. Moffat, J. Chromatogr. 120 (1976) 359.
[18] L.M. Jahangir, O. Samuelson, J. Chromatogr. 237 (1982) 371–379.
[19] P.R. Haddad, F. Hao, B. Glod, J. Chromatogr. 671 (1994) 3–9.
[20] J. Stahlberg, B. Jonsson, Cs. Horvath, Anal. Chem. 64 (1992) 3118–3124.
[21] C.M. Roth, K.K. Unger, A.M. Lenhoff, J. Chromatogr. A 726 (1996) 45–56.
[22] C.A. Brooks, S.M. Cramer, AIChE J. 38 (1992) 1969.
[23] C.A. Brooks, S.M. Cramer, Chem. Eng. Sci. 51 (1996) 3847.
[24] S.D. Gadam, G. Jayaraman, S.M. Cramer, J. Chromatogr. 630 (1993) 37.
[25] A.A Shukla, S.S. Bae, J.A. Moore, K.A. Barnthouse, S.M. Cramer, Ind. Eng. Chem. Res., submitted for publication.
[26] S. Udenfriend, S. Stein, P. Bohlen, W. Dairman, Science 178 (1972) 871.
[27] S. de Bernardo, M. Weigele, V. Toome, K. Manhart, W. Leimgruber, Arch. Biochem. Biophys. 163 (1974) 390.
[28] S. Siggia, Quantitative Analysis via Functional Groups, Wiley, Chichester, 1963, pp. 552–557.
[29] J. Bartos, M. Pesez, Pure Appl. Chem. 56 (1984) 467.
[30] R.S. Drago, T.R. Cundari, D.C. Ferris, J. Org. Chem. 54 (1989) 1042.
[31] E.M. Arnett, F.M. Jones, M. Taagepera, W.G. Henderson, J.L. Beauchamp, D. Holtz, R.W. Taft, J. Am. Chem. Soc. 94 (1972) 4724.
[32] R.R. Grinstead, J.C. Davis, J. Phys. Chem. 72 (1968) 1630.
[33] L.A. Truedsson, B.E.F. Smith, J. Chromatogr. 214 (1981) 291.
[34] J.P. Hickey, D.R. Passino-Reader, Environ. Sci. Technol. 25 (1991) 1753.
[35] R. Rosenfeld, K. Benedek, J. Chromatogr. 632 (1993) 29.